Accuracy of tropospheric and stratospheric water vapor measurements by the cryogenic frost point hygrometer: Instrumental details and observations

H. Vömel,[1,2] D. E. David,[1] and K. Smith[1]

[1] The cryogenic frost point hygrometer (CFH), currently built at the University of Colorado, is a new balloon borne hygrometer, which is capable of continuously measuring water vapor between the surface and the middle stratosphere. The design is loosely based on the old NOAA/CMDL frost point hygrometer, with improved accuracy and a number of significant new features that overcome some limitations of the older instrument. The measurement uncertainty of the new instrument depends on altitude and ranges between less than 4% in the tropical lower troposphere to no more than 10% in the middle stratosphere at 28 km. In the tropopause region the uncertainty is less than 9%. This instrument is used routinely at several sites for validation of satellite measurements and process studies in the upper troposphere and lower stratosphere region. It has proved to be particularly well suited for dehydration observations in the tropical upper troposphere, because the effects of cloud contamination have been significantly reduced. Results of this instrument are compared with the old NOAA/CMDL hygrometer, the Russian Fluorescent Lyman Alpha Stratospheric Hygrometer, the Vaisala RS92, the AURA/MLS satellite instrument, a cloud lidar, the NOAA/CSD frost point hygrometer and the Harvard Lyman-alpha hygrometer, both of the later instruments flown on board the NASA WB-57F high-altitude research aircraft. These comparisons demonstrate the level of accuracy of tropospheric and stratospheric water vapor measurements made by this instrument and point to areas where more research and development are needed.

1. Introduction

[2] Accurate in situ measurements of water vapor between the middle troposphere and the middle stratosphere remain a technical challenge. These measurements are important because of not only the strong impact of water vapor on our climate system but also the urgent need for validation of remote sensing observations from spaceborne or ground-based remote sensors. In situ measurements in the upper troposphere and lower stratosphere are typically obtained only with instruments on board high-flying research aircraft or expensive research balloon platforms. However, large discrepancies between instruments, even those on the same platform [*Kley et al.*, 2000], have made interpretation of the observations difficult. Radiosondes, depending on the manufacturer, generally provide useful data only in the lower and middle troposphere. Only a few techniques currently exist that allow frequent observations on small meteorological balloons and only one has been in use for an extended period of time. This instrument, a frost point hygrometer in regular use by NOAA/CDML for the last 26 years, is based on a design by *Mastenbrook and Dinger* [1960]. Its only major change occurred in 1979, when the stratospheric water vapor program was moved from the Naval Research Laboratory (NRL) to NOAA/ CMDL (now Global Monitoring Division of the NOAA/ Earth System Science Laboratory) in Boulder, Colorado. This instrument has been one of the most important tools for stratospheric water vapor measurements and has significantly contributed to our understanding of stratospheric water vapor [e.g., *Oltmans and Hofmann*, 1995; *Vömel et al.*, 1995, 2002]. However, because of its design, this instrument has been limited to measurements of stratospheric and middle to upper tropospheric water vapor, with upper tropospheric water vapor measurements being slightly less reliable than stratospheric measurements [e.g., *Vömel et al.*, 2007]. Furthermore, its design led to some variability in performance and made it unsuitable for large observation programs.

[3] An attempt was made to improve performance and reduce the size of this type of instrument by incorporating digital electronics [*Brown and Lichfield*, 1988], but it was abandoned despite some successful soundings (G. Brown,

[1] Cooperative Institute for Research in Environmental Sciences, University of Colorado, Boulder, Colorado, USA.
[2] Also at Global Monitoring Division, Earth System Research Laboratory, NOAA, Boulder, Colorado, USA.
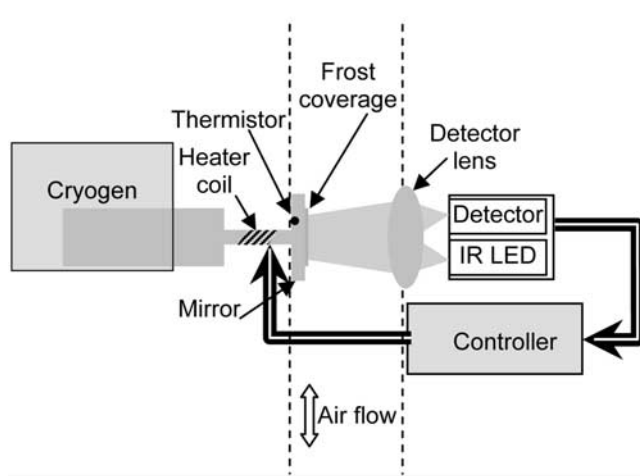
Figure 1. Schematic of the CFH sonde. The dashed lines indicate the vertical inlet tubes. The airflow inside the tubes is downward during balloon ascent and upward during descent. Only the lens and the mirror are exposed to the airflow inside the tube. The microprocessor controller regulates the mirror temperature such that the bulk reflectivity of the frost covered mirror remains constant.

personal communication, 2004). Therefore we have developed a new cryogenic frost point hygrometer (CFH) that overcomes most of the limitations of the NOAA/CMDL instrument and at the same time significantly reduces power consumption, weight, and cost. The CFH also requires less skill to operate and can be launched using smaller balloons, which is of great importance for the network of stratospheric and upper tropospheric water vapor sounding sites currently in preparation. Details of this instrument and its uncertainties, possible artifacts and characteristics are described below.

2. Instrument Description

[4] The instrument is based on the chilled-mirror principle: the temperature of a mirror is controlled such that it maintains a small and constant layer of condensate coverage (Figure 1). Under these conditions the mirror temperature equals the frost or dew point temperature of the air passing through the sensor. The mirror is connected to a cryogenic liquid (currently Trifluoromethane), which is able to cool the mirror to between 30°C and 100°C below any ambient frost point temperature. The mirror temperature is controlled by heating against this cold sink, which allows both fast heating and fast cooling rates. This cooling capacity avoids the low humidity limits faced by Peltier-cooled frost point instruments [e.g., *Vömel et al.*, 2003].

[5] The mirror disk is 1.27 mm thick with a diameter of 7 mm. The location of the thermistor is about 2 mm from the center of the mirror disk. The thermistor has a diameter of 0.46 mm and is glued into the mirror disk. The mirror and cold finger piece is machined from OFHC (oxygen free high conductivity) copper and gold plated.

[6] The frost or dew coverage on the mirror is detected by a photodiode that senses infrared light emitted by a

light-emitting diode (LED) and reflected off the mirror. A feedback controller uses the photodiode signal to control the heater and maintain the mirror temperature at the ambient frost point temperature. Several important features were incorporated into this new instrument that allow higher-accuracy measurements between the surface and roughly 25–28 km altitude in all climate regimes. Optimization of the mechanical and optical design as well as the use of a microprocessor instead of simple analog electronics led to significant weight savings and improved performance.

[7] The CFH weighs less than 400 g, including batteries (but excluding the cryogen), compared to more than 2000 g for the old NOAA/CMDL hygrometer. It is currently designed to be combined with ozone sondes to provide simultaneous profiles of water vapor and ozone. Launch preparations have been simplified significantly allowing any skilled balloon operator to launch this instrument. The instrument has a built in safety feature, which limits the mirror temperature to a maximum of 40°C. This feature prevents accidental burnout of the mirror heater, which may be caused by accidental misalignment of the optical path or foreign matter on either the lens or the mirror. Accidental burn out had also been a threat in humid tropical conditions if condensation formed on the detector lens after the instrument had been brought outside from an air-conditioned lab.

2.1. Condensate Detector

[8] The photodiode/LED pair used to detect the condensate coverage on the mirror surface is highly temperature sensitive and can lead to drift in the baseline signal. Temperature stabilization of the optical assembly largely eliminates this drift. To further reduce the temperature drift a second photodiode/LED pair is used in parallel and thermally connected to the first sensing pair. The photodiode of the reference path looks directly at the reference LED, and therefore compensates the residual thermal drift. The use of both thermal stabilization and the reference path makes the instrument less sensitive to changes in environmental conditions that arise from the wide range of climatic regions and solar heating that this instrument experiences.

[9] The optical path has been optimized. The core of the LED light spot and the area seen by the photodiode are centered on the inner 50% of the mirror surface. This eliminates the possibility of influences of the mirror edge on the frost detection.

[10] Since the CFH is intended for use during daytime as well as nighttime, sunlight has to be filtered out. The use of baffles, sun shields or other mechanical means to reduce ambient sun light at the detector was found to be not suitable, since any of these means are strong sources of contamination and affect the stratospheric part of the measurement. Baffles and sun shields also have been found to make the instrument highly sensitive to cloud contamination in particular in tropical soundings. Instead of mechanical shielding, a phase-sensitive detector was implemented to eliminate the solar contribution in the photodiode signal. The phase-sensitive detector is based on a switching device, which turns the LED on and off with a rate of 5 kHz, and calculates the difference between the photodiode signals with the LED turned on and the LED turned off.
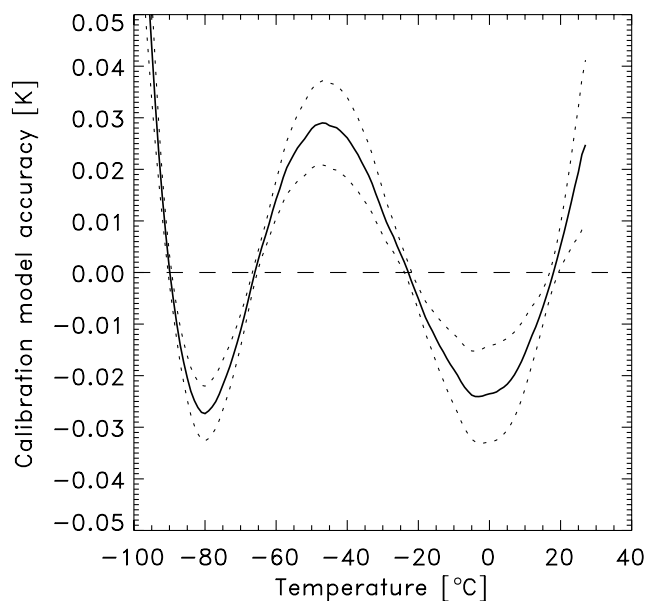
Figure 2. Difference between the calibration fit and the actually measured temperatures in a calibration run of 30 thermistors. The four calibration points are chosen to minimize the error at the warm and cold end of the temperature range.

This eliminates any solar influence on the condensate detection and allows a clean and highly sensitive control of the condensate coverage on the mirror.

2.2. Mechanical Integration and Contamination

[11] Figure 1 shows a representation of the geometry and orientation of all parts, although the parts are not to scale. The entire assembly is enclosed in an insulating foam box and only the inlet tubes are extending above and below the foam box. Clean sampling of ambient air is essential for water vapor observations in the upper troposphere and lower stratosphere. The CFH uses 17-cm-long stainless steel inlet tubes with a diameter of 2.5 cm and a wall thickness of 0.025 mm at the top and bottom of the instrument. These inlet tubes extend roughly 12 cm beyond the instrument in both directions and are exposed to sunlight. The thermal mass of these tubes is small and we believe that their temperature is close to ambient, except for solar heating, which will keep them warmer during daylight hours. We do not believe that there is a very large transfer of water vapor to and from these walls in the troposphere and lower-most stratosphere. We estimate that the flow through these tubes is roughly 50% of the balloon velocity. With a typical ascent velocity of 5 m/s the air passes through the inlet tube in about 70 ms. In most cases this is sufficient to minimize self contamination by the inlet tubes up to about 25 km altitude. Self contamination is negligible on descent because of the higher velocity of around 30 m/s to 60 m/s in the upper part of the descent and 15 m/s to 20 m/s in the tropopause region.

[12] The CFH is launched on small meteorological balloons, typically 1200 g rubber balloons for the combined CFH/ozone sonde payload. For this size balloon, contamination becomes noticeable above approximately 25–27 km,

even if the instrument is suspended 30 m below the balloon train. Flying through a moist troposphere can increase the balloon contamination somewhat, while a dry troposphere may allow clean sampling up to about 28 km on ascent. In the range between 20 km to 25 km balloon contamination is occasionally identifiable as very distinct peaks of high values as the swinging payload passes through the balloon wake. These contamination peaks are not reproduced on descent and are more severe if the instrument is suspended closer to the balloon. Contaminated observations, if present, are screened out in the data processing.

2.3. Thermistor Calibration and Data Transmission

[13] The mirror temperature is measured by a thermistor imbedded in the mirror disk. Each thermistor is individually calibrated to a NIST traceable standard over the temperature range +25°C to −100°C. A four point equation [adapted from *Steinhart and Hart*, 1968] is used to simplify the conversion from resistance to temperature. The calibration points are chosen such that the error is minimized over the range of expected frost point temperatures, about +25°C at the tropical surface to −94°C in the middle stratosphere or at the extreme tropical tropopause. The use of this equation introduces a systematic error not greater than 0.04°C for all mirror temperatures between −94°C and +25°C (Figure 2). At both the warm and the cold end of the temperature spectrum, this is a significant improvement over the previously used fixed three point calibration fit for the old NOAA/CMDL hygrometer [see *Vömel et al.*, 2007]. This improved fit is particularly relevant for measurements near the surface and the determination of the total water vapor column, as well as for middle stratosphere and cold tropical tropopause observations, where the calibration fit can be used without correction.

[14] Six standard thermistors are recalibrated in every calibration run of thirty thermistors. This helps to identify potential problems between calibration runs and can be used to establish the stability of the calibration procedure. So far, these thermistors have been recalibrated in ten different runs. Among all thermistors and all calibration runs, the resistances at four standard temperatures were reproduced to within 0.06% ± 0.5%. This uncertainty in the resistance measurement translates to an uncertainty in the temperature measurement of 0.007°C ± 0.03°C (1σ) over the entire temperature range. Therefore, on the basis of the recalibration of these six standard thermistors, we can assume that the uncertainty in the mirror temperature measurement introduced by the calibration procedure is less than 0.03°C at the 1 − σ level.

[15] The thermistor resistance is measured by a microcontroller using a 24 bit A/D converter. This minimizes the length of analog lines that this signal has to travel through and therefore the susceptibility to radiofrequency interference, which has been an issue in the past [*Vömel et al.*, 1995]. The mirror temperature is then transmitted digitally through the EnSci ozone sonde interface and the Vaisala RS80 radiosonde. The microcontroller code already applies the individual thermistor calibration to calculate the mirror temperature, eliminating the risk of operator error entering the wrong calibration coefficients. The effective resolution of the mirror temperature being transmitted to the ground is
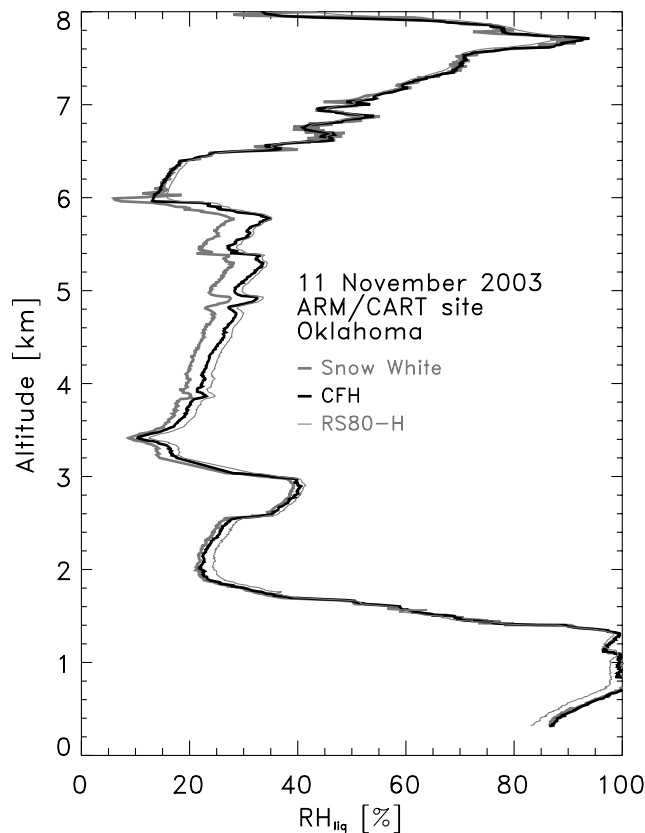
Figure 3. A sounding demonstrating the phase ambiguity of the mirror condensate in the Snow White instrument. This figure assumes ice on the Snow White mirror, which is an incorrect assumption below 6 km in this example. Using the appropriate liquid vapor pressure formulation in this region as in the CFH brings all three instruments into agreement.

14 bits or 0.01°C over the temperature range of −140°C to +50°C.

2.4. Physical Phase of the Mirror Condensate

[16] In the lower troposphere chilled mirror instruments inherently have to deal with an ambiguity in the phase of the condensate on the mirror. Instruments like the CFH, the Snow White hygrometer made by Meteolabor [*Vömel et al.*, 2003], and the old NOAA/CMDL frost point hygrometer can maintain liquid water as condensate on the mirror down to temperatures of −25°C to −30°C. The transition from liquid to frozen condensate happens spontaneously at temperatures that vary for each sounding. Therefore not knowing precisely the phase of the condensate may lead to an incorrect calculation of the water vapor pressure, since the phase of the mirror condensate, i.e., liquid or solid, determines the vapor pressure curve that has to be used to calculate the partial pressure of water in the air above the mirror [*Fujiwara et al.*, 2003]. Figure 3 shows as example a sounding using the Snow White hygrometer, a Vaisala RS92 radiosonde and the CFH, all on one balloon. The slight disagreement between the CFH and the Snow White hygrometer below 6 km is due to the ambiguity in the phase of the mirror condensate in the Snow White instrument. Figure 3

assumes ice on the mirror, which is an incorrect assumption for the Snow White below 6 km in this example. Using the appropriate liquid vapor pressure formulation in this region was found to bring all three instruments into agreement. Removing this ambiguity is of great importance. The CFH control algorithm eliminates this problem by force freezing the mirror condensate at a preset mirror temperature (currently −12.5°C), where the condensate is consistently liquid. At this temperature the mirror is allowed to cool to −38°C, which quickly freezes any liquid water on the mirror. After that normal control is resumed. This forced freezing leads to a data gap of typically 200 m or less and allows a clear identification of the liquid to ice transition. Mirror temperatures below the altitude where the force freezing occurs can then be interpreted unambiguously as dew point, and above this level as frost point.

[17] *Murphy and Koop* [2005] suggested that at very cold temperatures (T < 200 K) water ice may exist not only with its normal hexagonal crystal structure but also with a cubic crystal structure. They suggested that the vapor pressure of cubic ice may be 3% to 11% higher than that of hexagonal ice, which would influence frost point hygrometer measurements leading to colder frost point temperatures, if the condensate phase on the mirror was cubic ice instead of the normal hexagonal form. However, this is not expected to play a role in measurements using the CFH. Cubic ice is believed to be metastable under atmospheric conditions in the upper troposphere and lower stratosphere. The possibility exists that under very cold conditions cubic ice may form from the gas phase and persist for a period of time before spontaneously transforming to the stable hexagonal phase. However, it does not form from the stable hexagonal phase. The CFH evaporates and immediately reforms the frost layer at −53°C (220 K). At this temperature only hexagonal ice will form. The frost layer is then maintained into the colder region and will remain in the hexagonal phase, since a transformation to the metastable cubic phase is not possible under atmospheric conditions. Thus we do not expect that cubic ice plays a role in the way the CFH operates.

2.5. Feedback Controller

[18] The feedback controller is a digital proportional/integral/derivative (PID) controller, which uses a flexible parameter schedule to achieve optimal control over the entire expected frost point temperature range. The tuning of the PID controller is based on lab measurements, which were confirmed by atmospheric soundings. Whereas in the NOAA/CMDL hygrometer the gain change occurs only once in flight and lead to data loss of a few hundred meters to few km [*Vömel et al.*, 2007], the frequent and slight updating of the PID parameters in the CFH does not cause any loss of data. The PID schedule also makes the instrument settings independent of the geographic region in which the instrument is flown. CFH instruments can be launched with the same settings anywhere between polar and tropical regions. The PID parameters have been optimized for ascent measurements, which happen with a predictable and slow rise rate. The microprocessor includes a 16 bit pulse width modulator that drives the mirror heater and makes optimal use of the available battery power. The sensor draws about

Table 1. Sources of Measurement Uncertainty for the CFH

Source	Uncertainty
Controller stability	0.5°C
Thermistor calibration fit	0.04°C
Thermistor calibration reproducibility	0.03°C
Calibration of reference thermometer	0.02°C
Digitizing error	0.01°C
Temperature uniformity of the mirror	0.1°C
Total	0.51°C

3W continuous power, which is provided by small lithium batteries.

[19] The CFH controller maintains the reflectivity of an ice layer to within less than 0.3% (1σ), even in situations where the water vapor concentration changes rapidly. For liquid condensate the feedback controller is less stable in reflectivity, however, more stable in terms of temperature because of the higher amounts of water vapor. The significant improvements of the controller lead to much smaller oscillations of the mirror temperature around the ambient frost point temperature.

[20] The largest source of uncertainty in CFH water vapor measurements lies in the ability of the controller to maintain a constant condensate on the mirror. In most cases the feedback controller will lead to slight oscillations around the true frost point, which may have an amplitude of somewhere between 0.1°C for well behaved instruments to 1.0°C for slightly unstable instruments. The typical oscillation frequency in the stratosphere is around 25 s. For much larger oscillations that sometimes occur in the NOAA/CMDL frost point hygrometer, *Vömel et al.* [2007] have shown that these controller instabilities can be compensated by averaging. For the CFH we estimate the uncertainty introduced by the controller to be less than 0.5°C for 25 s averaged measurements even for slightly unstable instruments with oscillations of ±1.0°C. Given a typical ascent rate of 5 m/s, this uncertainty applies to layers of 125 m thickness. For well behaved instruments, this uncertainty is accordingly smaller and averaging is usually not needed. Further improvements in the feedback controller may lead to further improvements in the measurement accuracy.

2.6. Conversion of Mirror Temperature Into Relative Humidity and Mixing Ratio

[21] To convert frost point or dew point temperature measurements to relative humidity (RH) or mixing ratio, a vapor pressure equation is used to calculate the partial pressure of water vapor from the measured mirror temperature. For the sounding phase where ice is the condensate on the mirror (i.e., the middle troposphere and above), we use the Goff Gratch equation [*Goff and Gratch*, 1946]. This equation has been used by the NOAA/CMDL frost point hygrometer, in particular for the Boulder trend measurements. It agrees well with laboratory measurements by *Marti and Mauersberger* [1993], with differences of less than 2.3% at temperatures below −70°C. A recent review of vapor pressure formulations [*Murphy and Koop*, 2005] has pointed out that there is no experimental basis for giving preference to any of the widely used vapor pressure formulations over ice and that the measurement uncertainty currently is much larger than the uncertainty introduced by the use of any common vapor pressure formulations (over ice).

[22] The mixing ratio is calculated by dividing the water vapor partial pressure by the pressure of dry air. The uncertainty in mixing ratio is largely the same as that of the partial pressure, since the uncertainty of the absolute pressure is small except for the middle stratosphere (P < 20 hPa). The CFH currently uses the Vaisala RS80 pressure sensor, for which Vaisala claims an uncertainty of 0.5 hPa.

[23] To calculate relative humidity with respect to liquid water, great care has to be taken. Vaisala is the largest radiosonde manufacturer and uses the vapor pressure over liquid formulation by *Hyland and Wexler* [1983] in the calibration of their sensors. Since currently all CFH soundings carry a Vaisala radiosonde, this equation is used to assure consistency in the comparison with Vaisala RH measurements. The use of other vapor pressure formulations for vapor pressure over liquid will introduce additional differences at cold temperatures, when RH measurements are compared to Vaisala RH measurements. In particular the WMO recommended formulations [*World Meteorological Organization*, 1998, 2000] are highly problematic, since they contain typographical errors.

[24] A small correction exists for calculating the vapor pressure in moist air at high pressures compared to pure vapor. This enhancement factor amounts to roughly 0.5% at 1000 hPa [*Buck*, 1981]. Currently this enhancement factor is ignored to avoid inconsistencies with previous measurements. The error introduced by this is largely negligible compared to the measurement uncertainty and in particular it cancels out in the calculation of relative humidity.

2.7. Measurement Uncertainty

[25] Table 1 lists all uncertainties in the frost point or dew point measurement. The total uncertainty of the frost or dew point measurement is approximately 0.51°C. By far the dominating term is the controller stability and the value given here is a conservative estimate that covers most conditions. For liquid phase condensate the controller stability might actually be somewhat better than the value given here. This is in large part due to the higher amounts of water vapor, which make the instrument very sensitive to slight water vapor changes. However, at the same time the reflectivity stability is not as good as for the ice phase since small changes in temperature lead to rapid and large changes in reflectivity. Therefore the controller stability given in Table 1 should also be assumed for the liquid phase condensate.

[26] The second largest term of uncertainty is the uniformity of the mirror temperature and the location of the thermistor embedded in the mirror disk. Measurements with mirrors that had up to four thermistors installed at different locations indicate that the location of the thermistor does not play a role and that the mirror temperature was reproduced to within less than 0.1°C at all locations tested.

[27] The uncertainty in the air temperature measurement has to be considered in the uncertainty of RH [e.g., *Lin and Hubbard*, 2004]. All soundings currently use a Vaisala RS80 radiosonde, which provides the temperature measurement. The algorithm to derive the temperature from the Vaisala thermocap[®] response includes the radiation and ventilation correction provided by Vaisala. The random uncertainty in the temperature measurement is assumed to be 0.2°C, the accuracy stated by Vaisala. *Luers* [1997]
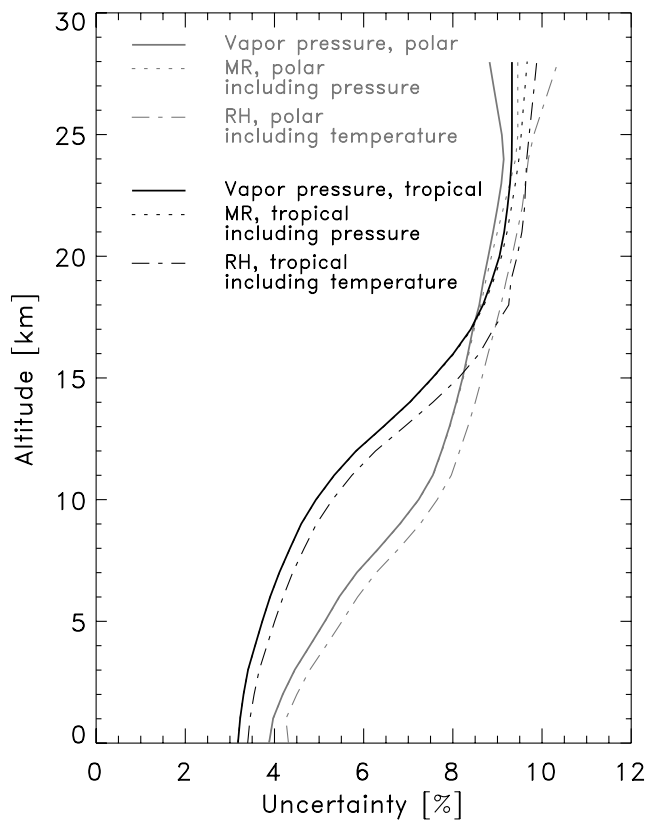
Figure 4. Measurement uncertainties derived from the frost point uncertainty as a function of altitude for typical tropical and polar soundings.

compared the RS80 and the RS90 temperature sensors and found that after correcting for solar heating the measurements of both sensors agreed to within 0.1 to 0.3°C. Our own comparisons between the RS80 and RS92 (successor to the RS90) obtained in 24 soundings at Alajuela, Costa Rica indicate that both agree to within <0.2°C throughout the entire troposphere and in the nighttime stratosphere and to within <0.3°C in the daytime stratosphere. Given the improved calibration for the RS92 as well as the much reduced radiation correction of the RS92, we see no reason to mistrust the stated accuracy of 0.2°C specified by Vaisala for the RS80 temperature measurements in the troposphere and tropopause region.

[28] Because of the nonlinearity of the vapor pressure equation, the uncertainty in the vapor pressure and therefore mixing ratio and relative humidity depend strongly on temperature and altitude as well as geographical region. Figure 4 shows the typical uncertainty of the vapor pressure, the mixing ratio and the relative humidity as a function of altitude for typical tropical and polar soundings. The uncertainty for the calculated mixing ratio shown in Figure 4 also includes a 0.5 hPa uncertainty in the pressure measurement, the accuracy stated by Vaisala. The contribution of this uncertainty is negligible in the troposphere and lower stratosphere, but becomes a significant contribution for the middle stratosphere.

[29] The RH uncertainty includes the uncertainty of 0.2°C in air temperature measurement and is expressed

as the % fraction of the RH; that is, a 4% uncertainty at saturation is equal to an uncertainty of 4% RH, whereas at an RH value of 10% this same 4% uncertainty of the RH percentage value is only 0.4% RH. The contribution of the air temperature uncertainty is small for the entire profile but is largest for the coldest part of the profile, typically the tropopause region. For a tropical noon time sounding, where the radiation error is largest, this contribution may be slightly larger at the tropical tropopause region.

[30] In a dual sounding on 13 December 2005, two CFH instruments were flown on the same payload to exclude the atmospheric variability as well as the pressure measurement uncertainty. These profiles are shown in Figure 5a. The difference between the measured frost point temperatures is less than 0.5°C throughout the entire ascent and most of the descent. Below 8 km on descent the frost point difference increases to more than 1°C. This payload was checked within 30 s after landing. Both instruments were found to be nearly out of cryogen and the difference on descent may be due to the cryogen running low earlier on one of the two instruments and subsequently less accurate frost point control. A higher battery voltage and a slightly higher optics voltage in this region may also be an indication of a low cryogen level on the last phase of the descent.

[31] While this sounding is consistent with the claimed uncertainty, it points out that great care has to be taken in interpreting the results and that attention to instrument parameters like frost coverage, optics signal and battery voltage is essential to properly interpret the measured mirror temperature.

[32] The AURA validation soundings during the Ticosonde 2005 campaign launched at Alajuela, Costa Rica are the first to make use of the phase-sensitive detector. Figure 6a shows the ascent and descent data of this campaign. Some obviously contaminated data have been eliminated. About 60% of the soundings (14 out of 24) can be used up to an altitude of 18 km and 37% (9 out of 24) are useful up to 25 km. Since the stratospheric variability is small, we can use these soundings to test whether the reproducibility of stratospheric water vapor observations is consistent with the uncertainties discussed here. Figure 6b shows a profile of the standard deviation in this set of soundings. The variability of these measurements includes the natural variability of water vapor in addition to all factors of uncertainty, including controller stability, calibration uncertainty and the uncertainty of the pressure measurement. Between 18 and 21 km the variability ranges between 8% and 11%, which is slightly larger than the instrumental uncertainty. Since this region is still dynamically very active, atmospheric variability is likely to contribute to the variability in the observations. Between 21 km and 25 km the variability (1σ) is about 6% and less than the instrumental uncertainty, while above 25 km it is slightly larger than the instrumental uncertainty. Since there is little reason to believe that the atmospheric variability is particularly large above 25 km, this result may indicate that balloon contamination becomes significant at this level. In a second field campaign at Biak, Indonesia, nine CFH sondes were launched daily in a period of 9 days and the variability of stratospheric water vapor in this data set shows the same result. The reproducibility of the CFH measurements in the stratosphere is consistent therefore with
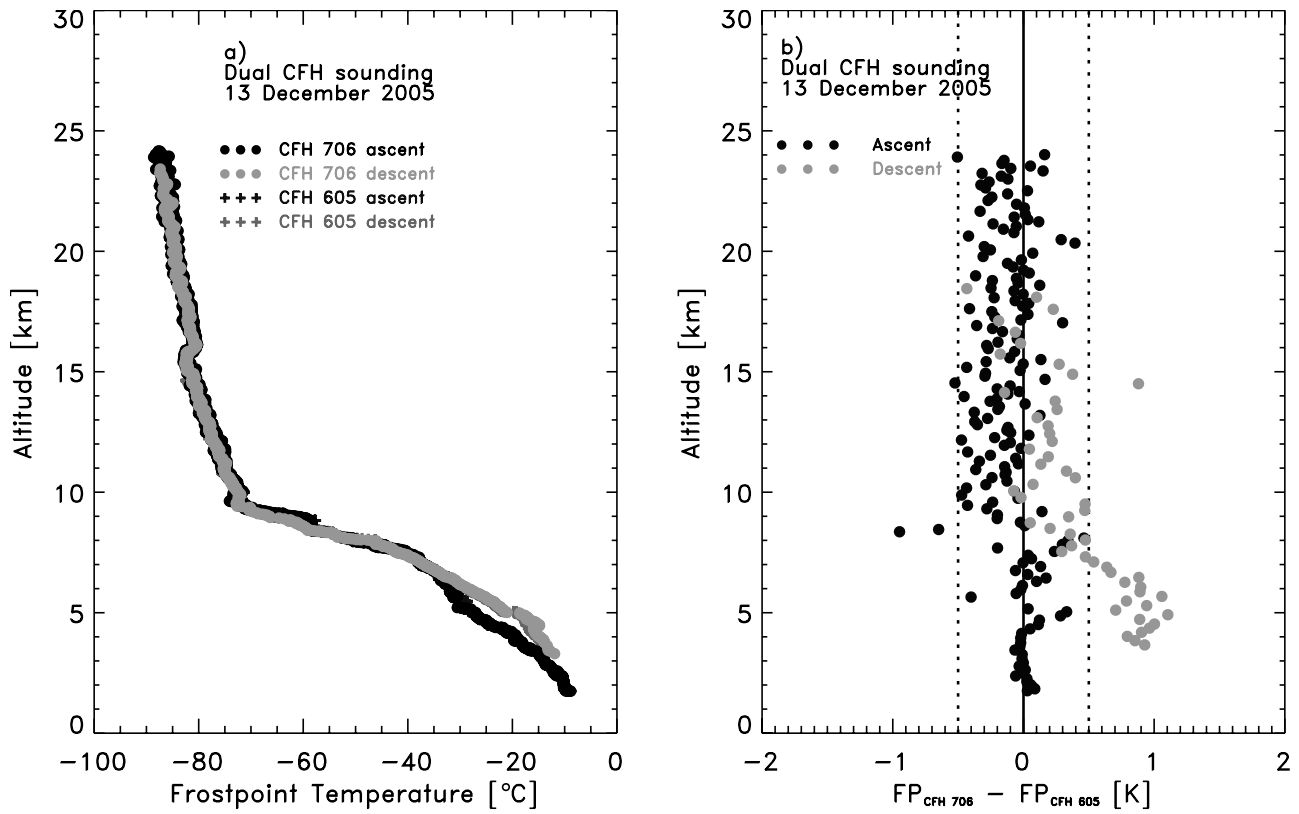
Figure 5. Direct comparison of two CFH instruments. (a) Profiles and (b) frost point difference.
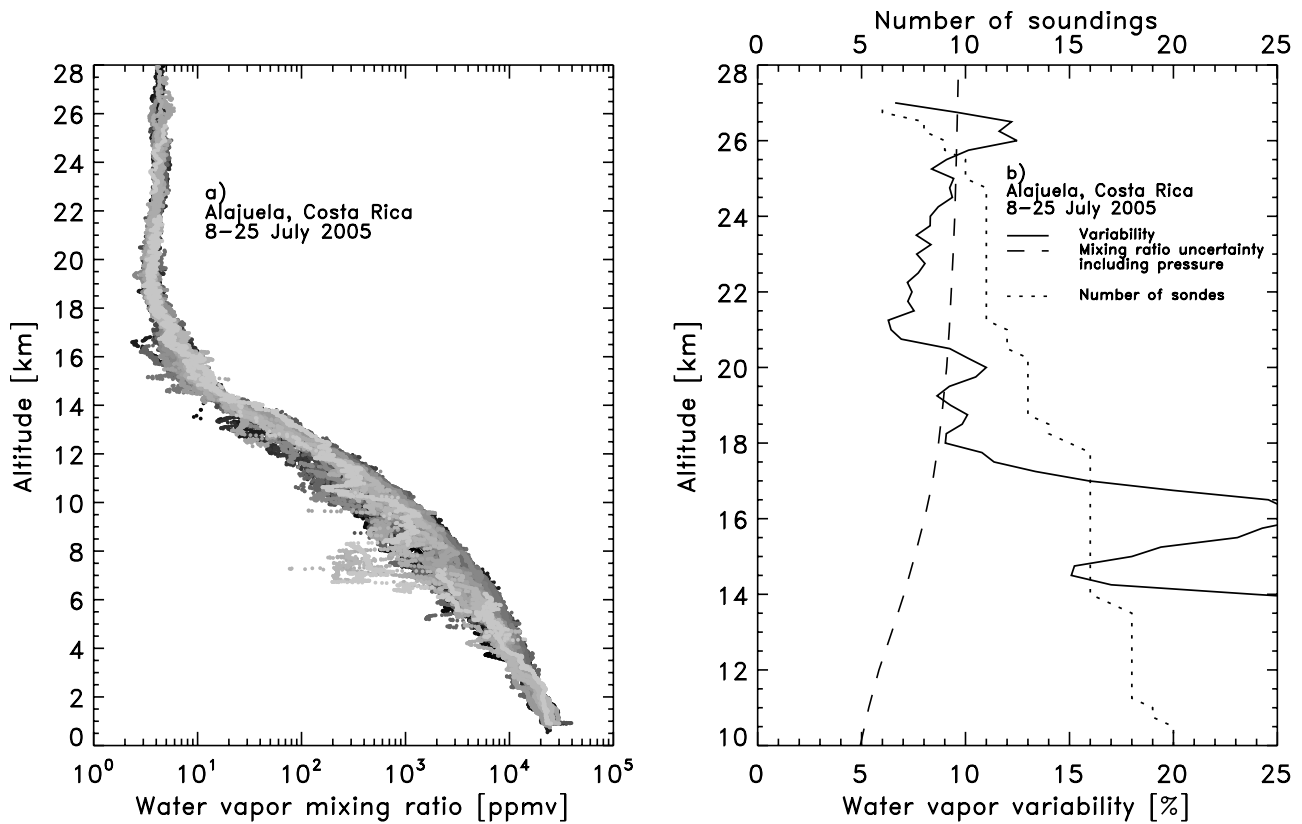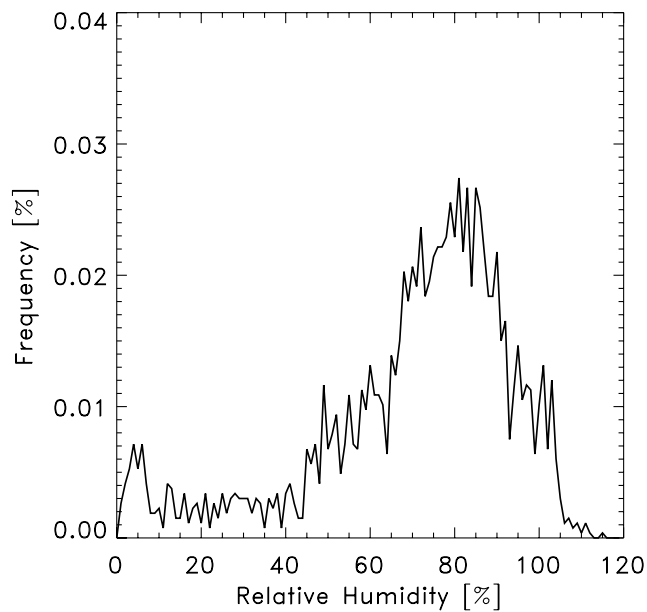

Figure 6. Profiles of soundings at Costa Rica between 8 and 25 July 2005. (a) Mixing ratio and (b) variability, mixing ratio uncertainty, and number of soundings.

Figure 7. RH frequency distribution for the 1–5 km layer in all soundings at Alajuela, Costa Rica.

the stated measurement uncertainty. Below the tropopause region this analysis is no longer valid, since the tropospheric variability becomes too large to test the reproducibility of the instruments.

[33] A reality check for the lower troposphere is the occurrence of liquid saturation in the lower troposphere, in particular for soundings that go through clouds. In liquid clouds we can expect that the relative humidity over liquid is very near 100% [e.g., *Korolev and Mazin*, 2003]. To be consistent with this threshold, which is determined by cloud physics, no observation within the measurement uncertainty should exceed this limit. In the tropical lower troposphere, the uncertainty in RH is about 3.4% of the measured RH value (Figure 4). For the entire Costa Rica data set, which so far contains 53 soundings, the RH over liquid frequency distribution in the layer below 5 km was calculated. This layer was chosen, since the 0°C level is at about 5 km and all clouds are liquid. To account for telemetry rate and ascent rate variations, all data were interpolated onto a 10 m grid. The RH frequency distribution (Figure 7) for this layer shows a sharp cutoff at 104% and a shallow tail extending to 110%. The RH frequency distribution is not a geophysically representative result and biased to lower values because of the fact that balloon launches in rain or under thick clouds were avoided; however, the sharp cutoff at 104% indicates that there is no low bias for lower tropospheric observations and at least no large high bias, if any, for lower troposphere observations. Furthermore, values of up to 4% above saturation are consistent with saturation within the instrumental uncertainty. Since the RH uncertainty is determined both by uncertainties in frost point temperature and in ambient temperature, it cannot be ruled out that the occasional high RH values (>104%) inside clouds are related to erroneously low temperature readings. This possibility exists since the temperature sensor inside clouds is constantly hit by liquid drops which are not in

thermal equilibrium with the surrounding air temperature. Drops colder than the surrounding air will lead to lower temperature readings and therefore higher RH readings, which could contribute to the tail of RH readings extending up to 110%. However, cloud contamination of the CFH through lens wetting (discussed below) cannot be ruled out for these cases either.

2.8. Observational Artifacts

[34] Several artifacts have been identified that may negatively affect a profile. At La Reunion and at Costa Rica, a small number of sondes have failed after being launched into precipitating or very wet clouds. Inside a cloud, liquid water may wet the lens of the optical detector, dramatically changing the detector signal. Under this condition the instrument ceases proper frost point control and heats the mirror to the maximum temperature as a result of wetting of the lens. Since the lens is at present unheated, this water film did not evaporate until the instrument had reached well into the stratosphere and at that point the instrument was unable to reform the frost coverage on the mirror in time.

[35] Several soundings at Costa Rica, at Tarawa, and at Biak showed a loss of frost point control in the upper troposphere close to the tropical tropopause. In these soundings the tropopause layer was highly supersaturated and condensation probably formed on the lens, with the same detrimental impact as wetting in liquid clouds. Since the tropical upper troposphere is usually close to saturation or supersaturated, this problem did not correct itself until the instrument has passed the tropopause and reached the warmer stratosphere. Furthermore, because of the low amounts of water vapor, frost point control was not regained until the instrument reached the upper troposphere on descent.

[36] Treating the lens surface with standard antifog coatings does reduce this effect, but the risk of lens condensation with subsequent loss of frost point control still remains. A lens heater has been developed and has successfully been tested in 13 soundings at Biak, Indonesia; Heredia, Costa Rica; and Beltsville, Maryland. These tests indicate that fogging of the lens may not be an issue in future soundings. However, the lens heater is not sufficiently strong to prevent wetting of the lens in liquid clouds.

[37] The quality of descent observations depends strongly on the descent velocity. The vertical velocity of a parachute descent in the stratosphere is usually 4 to 10 times faster than the ascent velocity, the upper part of the descent being the fastest. Typical descent rates at 30 km are between 40 m/s and 60 m/s, which places severe requirements on the PID tuning. It is nearly impossible to optimally tune the PID controller for the upper part of the parachute descent profile and we believe that because of this improper tuning, stratospheric descent data during parachute descent are often not as reliable as ascent measurements. The fact that in some soundings the controller is able to follow the rapidly changing water vapor points to the tuning of the instruments rather than another unidentified factor. Below the tropopause the descent velocity slows sufficiently, and the controller response rate increases, resulting in measurements that are just as reliable as they are on the ascent.

[38] In a few tropical soundings it was found that immediately after cooling started the battery power was tempo-

rarily insufficient to bring the mirror temperature to the ambient frost point and the mirror collected excessive amounts of liquid water. This problem corrected itself after launch, when the needed heater power dropped and the batteries strengthened. These data are easily screened out and this problem will be fixed with improved batteries.

2.9. Development History

[39] The instrumental features described so far reflect the present developmental stage of the CFH instrument. Several intermediate versions with slightly different performance characteristics have been used on some field campaigns. The first version of the CFH instrument used for the AIRS Water vapor Experiment (AWEX) in October and November 2003 did not yet have fully digital communication between the CFH and the EnSci interface. This partially analog instrument suffered from radio frequency interference (RFI), leading to a slight altitude-dependent offset. On these flights, the mirror temperature measurements were also stored in the flash memory of the microcontroller. Since these data were not subject to communications interference, they were used to correct this slight offset. A small residual error increased the uncertainty in frost point temperature measurement to 0.6°C. This campaign also used the same calibration equation as the NOAA/CMDL hygrometer; however, the additional uncertainty introduced is small since these soundings were launched in late fall with dew point temperatures at the surface near 0°C. Last the controller had not yet been properly tuned for stratospheric measurements, and the resulting data are considered reliable only up to the (midlatitude) tropopause.

[40] The instruments flown during the Soundings of Ozone and Water in Equatorial Regions (SOWER) at Bandung in December 2003 also used the analog data transmission, but, these instruments transmitted regular check values, which were later used to correct the RFI offset. These instruments were the first daytime launches of this instrument, and did not yet use phase-sensitive detection to eliminate the solar influence. In the upper troposphere and lower stratosphere, stray light from the sun caused significant controller instability and a much larger uncertainty in these measurements.

[41] During the LApbiat Upper Troposphere LOwer Stratosphere (LAUTLOS) water vapor experiment the fully digital data transmission was used for the first time. This introduced unexpected noise in the controller for stratospheric measurements, which has since been corrected.

[42] A sounding at Midland, Texas, in November 2004 was used in the comparison with the hygrometers on board the NASA WB-57F aircraft. This sounding was the first to use good stratospheric controller parameters, which have been largely unchanged since then. However, the phase-sensitive detector had not yet been implemented and baffles were used to reduce the solar influence. As a result, the ascent data in this sounding show high contamination. These data also show that baffles significantly reduce the airflow through the sensor and that contamination is flushed slowly from the sensor during the early phases of the descent.

[43] Beginning with the soundings at Boulder in June 2005 and the AURA validation soundings during the Ticosonde 2005 campaign launched at Alajuela, Costa Rica, all soundings have made use of the phase-sensitive detector,

eliminating the need for baffles. These soundings also implemented some minor improvements in the controller algorithm that further improved the frost point control in the upper troposphere and lower stratosphere. However, for testing purposes, the force freezing algorithm had been disabled in these instruments.

3. Intercomparisons
3.1. NOAA/CMDL Hygrometer

[44] The CFH is in parts based on the old NOAA/CMDL frost point hygrometer, and a comparison between the two instruments is needed to verify that there are no biases between the two instruments. The best comparison so far has been obtained with four soundings in June 2005, two soundings using the NOAA/CMDL hygrometer and two soundings using the new CFH. In these soundings the CFH made use of the phase-sensitive detector and provided good ascent data up to 25.6 km and good descent data during the fast balloon descent from 29 km. The NOAA/CMDL hygrometer soundings were launched on 7 and 30 June, the CFH soundings on 20 and 24 June. The meteorological conditions were very stable over this period and the stratospheric profiles are nearly identical. Figure 8a shows the descent profiles of these four soundings. Figure 8b shows the difference between the CFH profile on 20 June and the two NOAA/CMDL profiles on 7 and 30 June, as well as the difference between the CFH profile on 24 June and the two NOAA/CMDL profiles. Between 17.5 km and 23.5 km the differences between these four sondes is less than the instrumental uncertainty. Below 17 km the differences become meaningless because of the changes in the tropospheric and tropopause circulation as well as the tropospheric limitations of the NOAA/CMDL hygrometer. At 25 km the absolute difference between these soundings is 25% and decreases to 10% at 26.5 km, which is most likely a true difference in the atmospheric circulation and not an instrumental artifact. Therefore these four soundings do not suggest any bias of the CFH compared to the NOAA/CMDL hygrometer in the stratosphere although a more rigorous comparison is still to be done. These soundings also indicate that the CFH is capable of obtaining good observations during a fast parachute descent, compared to the necessary slow valved descent on the old NOAA/CMDL hygrometer.

3.2. FLASH-B

[45] The LApbiat Upper Troposphere LOwer Stratosphere (LAUTLOS) project in February 2004 studied the performance of several balloon borne water vapor instruments in the polar atmosphere and in particular the comparison between the NOAA/CMDL hygrometer and the Fluorescent Lyman-α Stratospheric Hygrometer for Balloons (FLASH-B) of the Central Aerological Observatory. This project showed generally a good agreement between these two balloon-borne stratospheric water vapor instruments [*Vömel et al.*, 2007]. The CFH soundings launched during LAUTLOS did not yet provide useful stratospheric data because of several technical difficulties at that early stage. However, a sounding on 19 December 2005 at Sodankylä, Finland provided simultaneous data of the CFH and the FLASH-B on the same balloon payload. Figure 9a shows the descent section of both soundings.
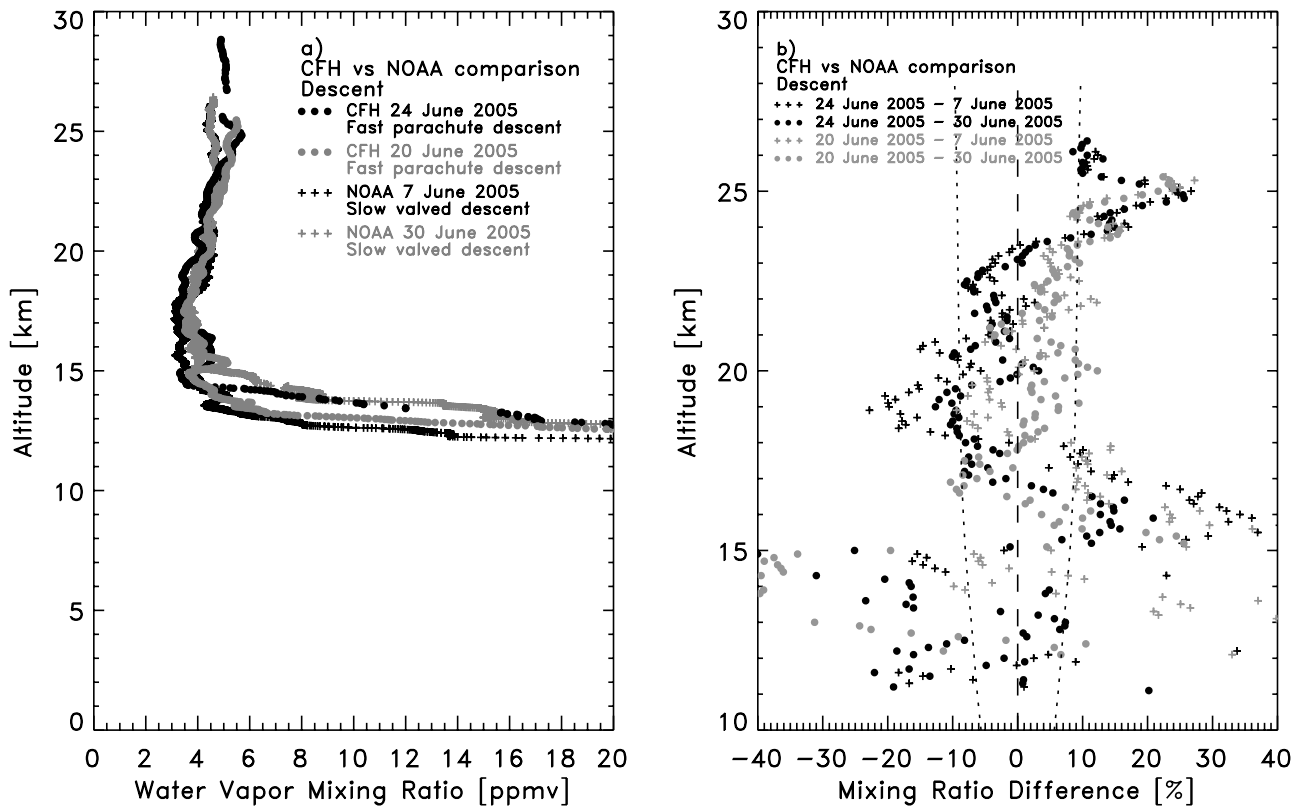
Figure 8. Profiles by the NOAA/CMDL hygrometer and the new CFH on 4 days in June 2005. (a) Mixing ratios and (b) difference between CFH and NOAA/CMDL sondes. Dashed lines indicate measurement uncertainty.
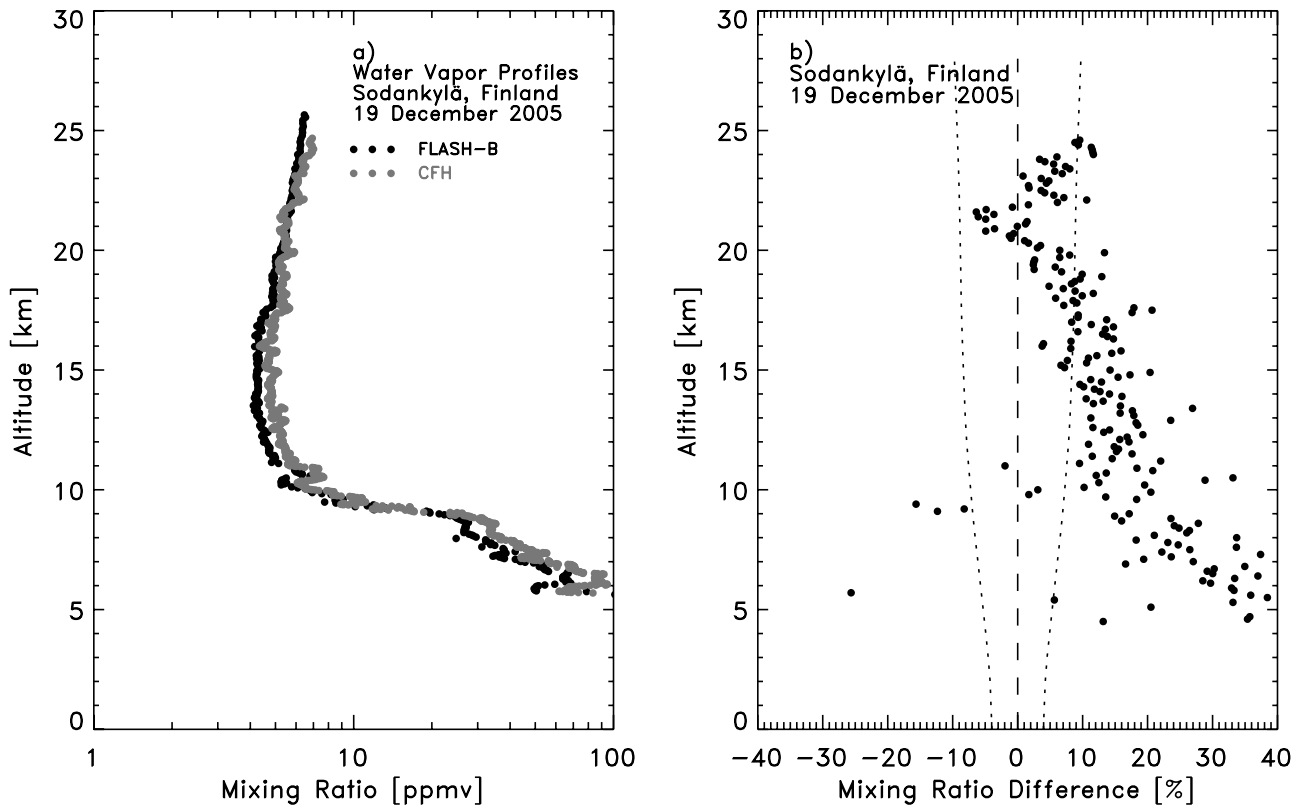
Figure 9. Comparison between FLASH-B and CFH at Sodankylä, Finland, 19 December 2005. (a) Individual profiles and (b) CFH − FLASH difference. Dashed lines indicate measurement uncertainty.
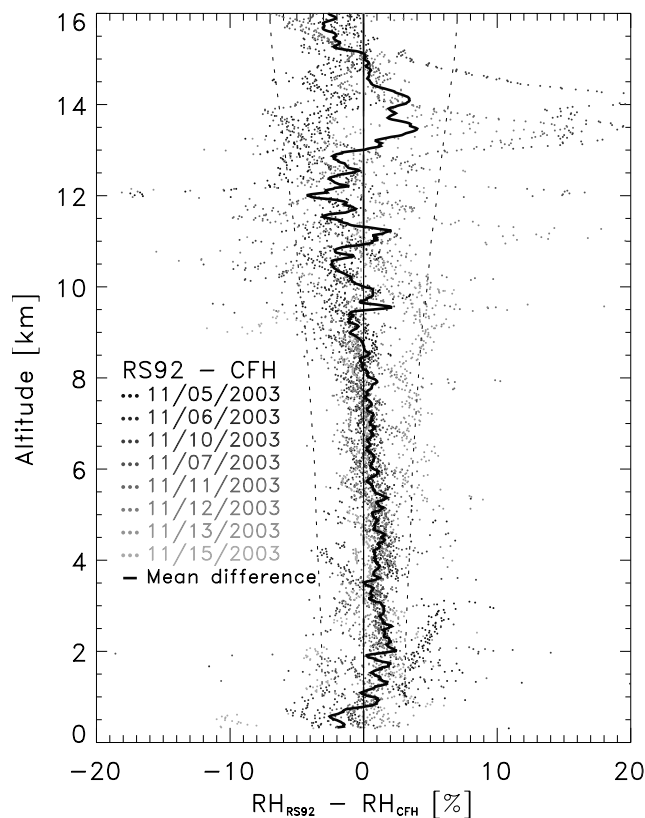
Figure 10. Relative humidity difference between the Vaisala RS92 radiosonde humidity sensor and the CFH relative humidity from eight soundings during AWEX, 5–15 November 2003. Dashed lines indicate measurement uncertainty.

This sounding shows significant differences between the ascent and descent profiles, indicative of contamination likely due from the larger plastic balloon compared to the contamination from the usually smaller rubber balloons. The larger payload and larger loadline may also have contributed to these differences.

[46] Most features of the profile are well reproduced in both instruments; however, in the altitude range between 7 and 25 km the FLASH instrument shows lower values compared to the CFH. Below 7 km the comparison is meaningless since the FLASH loses signal [*Vömel et al.*, 2007]. Since the difference is increasing with decreasing altitude (Figure 9b), contamination can be ruled out as the source for this disagreement. The CFH response improves with the slowing of the parachute at lower altitude and CFH controller problems are not suspected. However, the FLASH calibration has shown to be stable and is also an unlikely explanation (S. Khaykin, personal communication, 2006). A second CFH sounding on 20 December shows better agreement with the FLASH data on 19 December. Since the stratospheric circulation was stable during these 2 days, the better agreement with the sonde on 20 December might indicate an unidentified instrumental issue with the sonde launched on 19 December. There is currently no good explanation for this disagreement and it remains under investigation.

3.3. RS92

[47] CFH sondes have been flown in 12 soundings during AWEX at the ARM/CART site near Lamont, OK and were used to evaluate the performance of other radiosonde sensors, e.g., the RS80, RS90, and RS92 radiosondes from Vaisala as well as the Snow White hygrometer from Meteolabor. Here only the comparison with the RS92 is shown (Figure 10), since these were the first RS92 soundings launched in North America. All soundings were launched at night and show a very good agreement between the RS92 and CFH relative humidities. The mean difference is less than 3% RH throughout the entire troposphere. A small drying of the RS92 values compared to the CFH between the surface and 10 km has been identified and a correction has been determined by *Miloshevich et al.* [2006].

3.4. MLS

[48] The soundings at Alajuela, Costa Rica have all been launched at nominal AURA/MLS overpass times although no attention has been paid to the distance of the overpass. Figure 11 shows all CFH water vapor profiles and all AURA/MLS water vapor profiles in a box of ±20° longitude and ±5° latitude during the same period. These soundings indicate an excellent agreement between MLS satellite observations and the CFH above 100 hPa and a dry bias for MLS in the upper troposphere. The difference of the averages of these two sets of data shows a possible dry bias for AURA.MLS of up to 40% at 216 hPa. The large
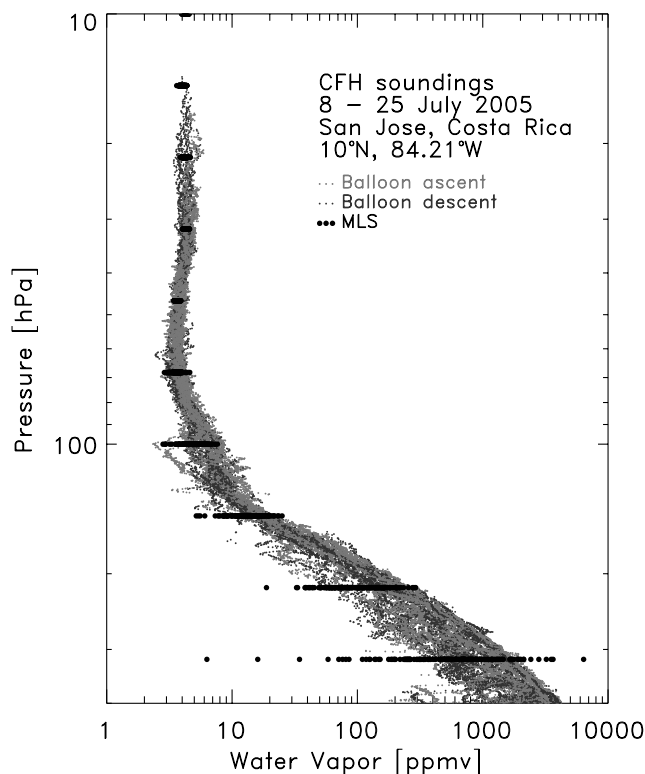
Figure 11. CFH profiles at Alajuela, Costa Rica, between 8 and 25 July 2005 and AURA/MLS water vapor retrievals in a box of ±20° longitude and ±5° latitude around the launch site during the same period.
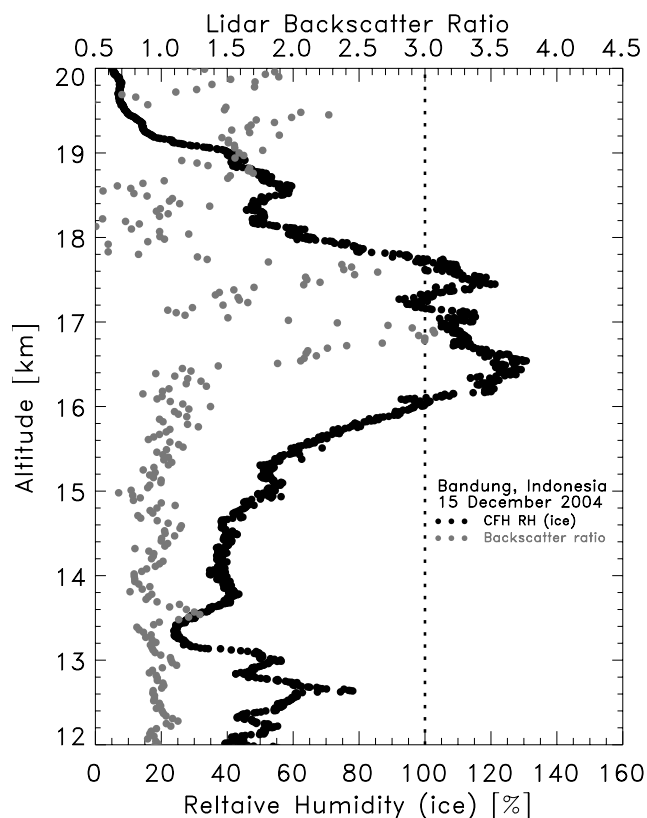
Figure 12. Relative humidity with respect to ice and lidar backscatter ratio at Bandung, Indonesia, 15 December 2004.

scatter of the MLS observation in the upper troposphere may be indicative of a larger natural variability in this altitude region. However, even in carefully matched and cloud free comparisons, the MLS-CFH difference shows a large scatter indicative of possible retrieval problems in the upper troposphere. The details of these comparisons go beyond the current paper and will be discussed elsewhere.

3.5. Lidar

[49] On 15 December 2004 at Bandung, Indonesia a sounding was launched in conjunction with lidar observations of tropopause cirrus clouds. Figure 12 shows the profile of relative humidity, water vapor mixing ratio and backscatter ratio. This sounding shows that regions of high supersaturation in the tropical tropopause region may also contain ice clouds, therefore actively contributing to dehydration in the tropical tropopause layer. The CFH humidity profile shows ice supersaturation between 16.1 km and 17.7 km with a brief drop below ice saturation at 17.3 km. The lidar detected ice particles between 16.4 km and 17.7 km with a shallow nearly clear layer at 17.3 km. The RH peak is at 16.4 km with a value of 128%. This is just at the lower edge of the cirrus cloud and possibly an indication for a RH threshold required for the formation of cirrus clouds in the tropical tropopause region. While the frequency of this correlation remains to be quantified, this observation supports the assumption that the observations of high values of ice supersaturation may be an indicator for active dehydra-

tion. The details of this observation are discussed at length elsewhere [*Shibata et al.*, 2007].

3.6. WB-57 Midland Sounding

[50] On 18 November 2004 a balloon launch at Midland, Texas, was coordinated with water vapor measurements on board NASA's WB-57F high-altitude research aircraft. In this experiment the WB-57F spiraled from 18 km to 12.5 km and back up to 18 km during the balloon ascent and again during the balloon descent. Two water vapor instruments on board the WB-57, the Harvard Lyman-α hygrometer and the new NOAA/CSD aircraft frost point hygrometer provided data during this experiment. This flight was another attempt to address the long-standing issue of disagreements between various in situ instruments that measure water vapor in this altitude region.

[51] Figure 13 shows the descent profile of the CFH and all descent and ascent profiles of the WB-57F instruments. The CFH flown in this experiment did not yet have the phase-sensitive detector and used baffles to shield the detector from sunlight. This led to severe contamination on ascent and, because of the reduced airflow through the inlet tubes, the instrument responded slightly slower and showed some contamination on descent after the balloon burst. However, in the region of the aircraft observations contamination on descent did not play a role. The three instruments show some disagreement, with the NOAA/CSD frost point hygrometer showing good agreement with the
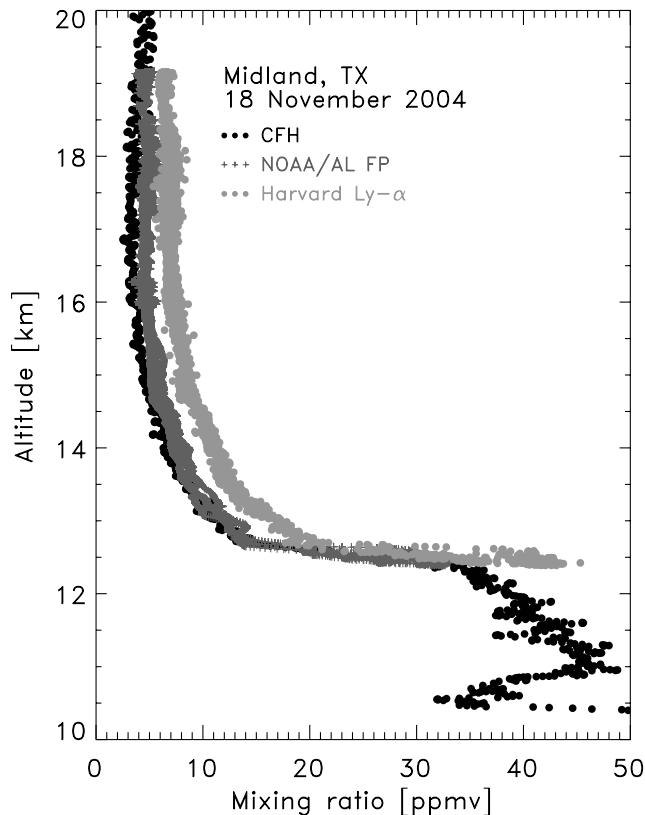
Figure 13. Comparison between CFH and the WB-57F instruments Harvard Lyman-α and NOAA/CSD frost point hygrometer.

CFH at 19 km and below 14 km and values up to 40% higher at 17 km. Throughout the entire altitude region, the Harvard Lyman-α show values between 50% and 110% above those measured by the CFH. Since the uncertainty for the Harvard instrument is 5% [*Hintsa et al.*, 1999] and the uncertainty for the CFH in this altitude region between 8% and 9%, this large discrepancy cannot be explained by instrumental uncertainty.

[52] While there is no clear indication for the source of this difference, the closer agreement of the two frost point instruments may indicate that the difference is not related to the measurement platform, but rather to the techniques or instrumental implementations of the technique.

[53] Disagreements between aircraft borne instruments and balloon borne instruments have been reported in the past [*Kley et al.*, 2000], and the comparison presented here reinforces the need to address this issue in more detail.

4. Summary and Conclusion

[54] The Cryogenic Frost point Hygrometer (CFH), developed at the University of Colorado, is a small light-weight balloon-borne hygrometer capable of measuring water vapor between the surface and the middle stratosphere. It is based on a simple physical principle that has been used on balloon platforms for several decades. The current improvements of this technology make this instrument highly suitable for process studies in the upper troposphere and lower stratosphere, particularly for the tropical tropopause region and for the polar stratosphere, as well as for long-term trend studies of water vapor in the troposphere and stratosphere. It is also considered as reference instrument for the validation of spaceborne and ground-based remote sensors as well as radiosonde humidity sensors. The design is well suited for water vapor measurements inside ice clouds and even tolerates some contamination in liquid clouds.

[55] The current configuration makes use of the EnSci ozone sonde interface and is intended to be flown together with ozone sondes. The combination of these two trace gases provides a powerful tool to study a large variety of atmospheric processes. Because of better availability, ease of operation and highly improved performance, the creation of a network of stations that routinely conduct balloon borne soundings of water vapor and ozone from the surface to the middle stratosphere is now within reach.

[56] The comparison with the NOAA/CMDL frost point hygrometer as well as with AURA/MLS show excellent consistency and do not give any indication for a bias of either instrument in stratospheric water vapor measurements. The observations within clouds in the lower troposphere as well as within cirrus clouds are consistent with cloud physics and support the measurement uncertainties. A possible slight wet bias observed in the comparison with FLASH-B may have been an artifact of that particular instrument and was not reproduced in a follow up sounding. The disagreement the Lyman alpha hygrometer of Harvard University and the CFH repeats similar results between the Harvard Lyman alpha instrument and the NOAA/CMDL frost point hygrometer, which points to the urgent need to resolve this disagreement.

[57] The results here indicate the level of accuracy to which atmospheric water vapor can be measured by balloon borne frost point hygrometers and will help to constrain the amount of upper tropospheric and stratospheric water vapor concentrations derived from such observations.

References

Brown, G. S., and E. W. Lichfield (1988), A balloon-borne frost point hygrometer for tropospheric and stratospheric water vapor concentration measurements, *SAND88-2467*, Sandia Natl. Lab., Albuquerque, N. M.
Buck, A. L. (1981), New equations for computing vapor pressure and enhancement factor, *J. Appl. Meteorol.*, *20*, 1527–1532.
Fujiwara, M., M. Shiotani, F. Hasebe, H. Vömel, S. J. Oltmans, P. W. Ruppert, T. Horinouchi, and T. Tsuda (2003), Performance of the Meteolabor "SnowWhite" chilled mirror hygrometer in the tropical troposphere: Comparisons with the Vaisala RS-80 A/H humicap sensors, *J. Atmos. Oceanic Technol*, *20*, 1534–1542.
Goff, J. A., and S. Gratch (1946), Low-pressure properties of water from −160 to 212 F, *Trans. Am. Soc. Heating Ventilating Eng.*, *52*, 95–122.
Hintsa, E. J., E. M. Weinstock, J. G. Anderson, R. D. May, and D. F. Hurst (1999), On the accuracy of in situ water vapor measurements in the troposphere and lower stratosphere with the Harvard Lyman-α hygrometer, *J. Geophys. Res.*, *104*, 8183–8190.
Hyland, R. W., and A. Wexler (1983), Formulations for the thermodynamic properties of the saturated phases of H_2O from 173.15 K to 473.15 K, *Trans. Am. Soc. Heating Refrigeration Air-Conditioning Eng.*, *89*, 500–519.
Kley, D., J. M. Russell III, and C. Philips (2000), SPARC assessment of upper tropospheric and stratospheric water vapour, WCRP 133, WMO/TD No. 1043, *SPARC Report 2*, 312 pp., World Clim. Res. Prog., World Meteorol. Org., Geneva.
Korolev, A. V., and I. P. Mazin (2003), Supersaturation of water vapor in clouds, *J. Atmos. Sci.*, *60*, 2957–2974.
Lin, X., and K. G. Hubbard (2004), Uncertainties of derived dew point temperature and relative humidity, *J. Appl. Meteorol.*, *43*, 821–825.
Luers, J. K. (1997), Temperature error of the Vaisala RS90 radiosonde, *J. Atmos. Oceanic Technol.*, *14*, 1520–1532.
Marti, J., and K. Mauersberger (1993), A survey and new measurements of ice vapor pressure at temperatures between 170 and 250 K, *Geophys. Res. Lett.*, *20*, 363–366.
Mastenbrook, H. J., and J. E. Dinger (1960), The measurement of water vapor distribution in the stratosphere, *Tech. Rep. NRL 5551*, 35 pp., Nav. Res. Lab., Washington D. C.
Miloshevich, L. M., H. Vömel, D. N. Whiteman, B. M. Lesht, and F. J. Schmidlin (2006), Absolute accuracy of water vapor measurements from six operational radiosonde types launched during AWEX and implications for AIRS validation, *J. Geophys. Res.*, *111*, D09S10, doi:10.1029/2005JD006083.
Murphy, D. M., and T. Koop (2005), Review of the vapour pressures of ice and supercooled water for atmospheric applications, *Q. J. R. Meteorol. Soc.*, *131*, 1539–1565.
Oltmans, S. J., and D. J. Hofmann (1995), Increase in lower-stratospheric water vapour at a midlatitude Northern Hemisphere site from 1981 to 1994, *Nature*, *374*, 146–149.
Shibata, T., H. Vömel, S. Hamdi, S. Kaloka, F. Hasebe, M. Fujiwara, and M. Shiotani (2007), Tropical cirrus clouds near cold point tropopause under ice supersaturated conditions observed by lidar and balloon-borne cryogenic frost point hygrometer, *J. Geophys. Res.*, *112*, D03210, doi:10.1029/2006JD007361.
Steinhart, I. S., and R. Hart (1968), Calibration curves for thermistors, *Deep Sea Res.*, *15*, 497–503.
Vömel, H., S. J. Oltmans, D. J. Hofmann, T. Deshler, and J. M. Rosen (1995), The evolution of the dehydration in the Antarctic stratospheric vortex, *J. Geophys. Res.*, *100*, 13,919–13,926.

Vömel, H., et al. (2002), Balloon-borne observations of water vapor and ozone in the tropical upper troposphere and lower stratosphere, *J. Geophys. Res.*, *107*(D14), 4210, doi:10.1029/2001JD000707.

Vömel, H., M. Fujiwara, M. Shiotani, F. Hasebe, S. J. Oltmans, and J. E. Barnes (2003), The behavior of the Snow White chilled-mirror hygrometer in extremely dry conditions, *J. Atmos. Oceanic Technol*, *20*, 1560–1567.

Vömel, H., V. Yushkov, S. Khaykin, L. Korshunov, E. Kyrö, and R. Kivi (2007), Intercomparisons of stratospheric water vapor sensors: FLASH-B and NOAA/CMDL frost point hygrometer, *J. Atmos. Ocean. Technol*, in press.

World Meteorological Organization (1998), General meteorological standards and recommended practices, Appendix A, *WMO Technical Regulations, WMO-no. 49*, World Meteorol. Org., Geneva.

World Meteorological Organization (2000), General meteorological standards and recommended practices, Appendix A, *WMO Technical Regulations, WMO-no. 49, Corrigendum*, *August 2000*, World Meteorol. Org., Geneva.

———————————

D. E. David, K. Smith, and H. Vömel, Cooperative Institute for Research in Environmental Sciences, University of Colorado, Boulder, CO 80309-0216, USA. (holger.voemel@colorado.edu)